Initial testing of a Si:As blocked-impurity-band (BIB) trap detector

Solomon I. Woods[a], Simon G. Kaplan[a], Timothy M. Jung[b], Adriaan C. Carter[c] and James E. Proctor[d]

[a]National Institute of Standards and Technology, 100 Bureau Drive, Gaithersburg, MD, USA 20899;
[b]Jung Research and Development Corp., 1706 U St. NW #204, Washington, DC, USA 20009;
[c]Booz Allen Hamilton Inc., One Preserve Parkway, Suite 200, Rockville, MD, USA 20852;
[d]Jeptech, Inc, PO Box 4220, Gaithersburg, MD 20885

ABSTRACT

We discuss the design, construction, and initial test results of a Si:As blocked-impurity-band (BIB) trap detector. The trap consists of two rectangular BIB devices configured in a v-shaped geometry. This trapping geometry is designed to ideally yield a minimum of 7 bounces before exit for incident light within an f/4 cone with 3 mm clear aperture. The individual BIB devices consist of 70 µm thick active layers with As doping near 1.7×10^{18} cm^{-3}, and have dark currents of approximately 100 nA at an operating temperature of 9 K. A simple ray-tracing model of the trap, along with data on the quantum yield of typical BIB detector elements, indicates that it is possible to achieve an external quantum efficiency of > 0.99 over the 4 µm to 28 µm spectral range and significant suppression of the etalon fringes present in the spectral responsivity of a single element. We have made initial responsivity measurements of the trap compared to a calibrated 5 mm diameter pyroelectric detector over the 3 µm to 17 µm spectral range using the fiber-coupled output of a Fourier-transform spectrometer. We also discuss the results of comparison measurements between the trap detector and an absolute cryogenic radiometer viewing the output of a calibrated blackbody source at discrete filter bands from 5 µm to 11 µm. In initial testing the performance of the trap is limited by the poor performance of the individual BIB detectors, but the advantages of boosted quantum efficiency and suppressed etalon are realized by the trap.

Keywords: BIB detector, blocked-impurity-band detector, trap detector, infrared detector, long wavelength IR detector, far infrared detector, detector calibration

1. INTRODUCTION

Blocked impurity band (BIB) detectors based upon doped semiconductors provide high performance detection and imaging in the infrared [1-3]. BIB detectors are of crucial importance for optical calibration, military applications and astronomical measurements in the wavelength range from 2 µm to 30 µm, and they have the potential for measurements in the far infrared out to 1 mm [4]. The National Institute of Standards and Technology (NIST) uses BIB detectors as the basis for transfer of low-power infrared (IR) standards [5-7]. BIB detectors must in general be operated at cryogenic temperatures but offer low noise in addition to high responsivity, speed, linearity and spatial uniformity [8].

BIB detectors exhibit excellent responsivity in the long wavelength infrared (LWIR), but they also present some disadvantages for use as a standard reference detector. BIB detectors are thin film devices generally fabricated on silicon substrates, so they exhibit significant etalon in their infrared spectral response, caused by the interference of multiply reflected light between the surfaces of the detector [9]. The large amplitude, short period spectral features caused by the etalon (as well as some absorption lines in the silicon substrate) make it difficult to use BIB detectors for accurate spectral calibrations at single wavelengths and also increase the uncertainty in broadband spectral calibrations made over filter bands. Another problem with the typical backside-illuminated BIB detector is that overall quantum efficiency of the device is limited in general to 60 % or less because there is significant reflectance loss at the detector surface, internal quantum efficiency loss through the detector substrate, and less than 100 % absorption through the depth of the thin infrared-active layer.

We have developed a BIB trap detector, fabricated with individual BIB devices custom-designed to exhibit low internal losses and high absorptivity, to minimize the etalon and maximize the quantum efficiency associated with BIB devices. The trap detector is composed of two Si:As BIB devices in a v-shaped geometry and is designed such than an f/4 beam

Infrared Technology and Applications XXXVIII, edited by Bjørn F. Andresen, Gabor F. Fulop, Paul R. Norton,
Proc. of SPIE Vol. 8353, 83533G · © 2012 SPIE · CCC code: 0277-786X/12/$18 · doi: 10.1117/12.919563

passing through a 3 mm aperture near the detectors will ideally bounce seven times within the trap before reemerging. As the beam progresses through the trap, striking each detector multiple times at different angles, the etalon structure of the absorption is averaged out and the total absorption increases as well. For this application, we have had low internal loss BIB devices, with relatively thick active layers for improved absorptivity, custom-designed and fabricated. It is predicted that a trap of this design, made from BIB devices with thick active layers and low internal losses, should exhibit a smooth spectral response with quantum yield greater than 99 % over the wavelength range from 4 μm to 28 μm.

Initial testing of our first BIB traps are promising, but show limitations due to the poor performance of the individual new BIB devices fabricated for this project. Comparison of the response of a BIB trap with a single BIB device shows that the trapping arrangement removes nearly all trace of etalon and significantly boosts the quantum yield. The single new BIB devices, used for the trap, however, exhibit much lower quantum efficiency than typical Si:As BIBs, so the quantum yield of the trap is significantly lower than predicted for the ideal case. As of yet, measurements of the trap have only been made from 3 μm to 17 μm, so longer wavelength measurements are still required to determine the spectral response of the trap over the full sensitivity range of its BIB detectors.

2. DESIGN OF THE BIB TRAP

We modeled the trap geometry with varying angles of incidence and wedge angle to determine the optimum configuration to minimize detector area and maximize absorption. The results of the modeling led to the adoption of a 49° angle of incidence at the first detector and a 14° wedge angle. The detectors for this trap require approximate dimensions of 10.2 mm × 8.2 mm. The beam size and beam location for the seven bounces through the trap, superimposed on the schematic of a single detector, are displayed in Figure 1. Assuming that each BIB detector in the trap exhibits a spectral absorptivity achieved by typical Si:As BIB detectors, the total quantum efficiency for a trap of our design with low internal loss detectors can be estimated. The estimated quantum efficiency for such a trap is shown in Figure 2.

The mechanical design of the trap assembly aims to minimize strain on the BIB detectors as the trap is cooled to cryogenic temperatures, and the design is organized for flexible and modular assembly. The trap mount was machined from Invar, which has a very small coefficient of thermal contraction, similar to the silicon of the detectors. The mount was plated with gold to minimize radiative heating of the trap assembly and to protect the Invar from corrosion. Each BIB device was mounted on a silicon frame, with a polyimide flex circuit epoxied to the frame. The frame and flex circuit provide a useful platform for arranging and wirebonding the detector and then the frames can be epoxied to the

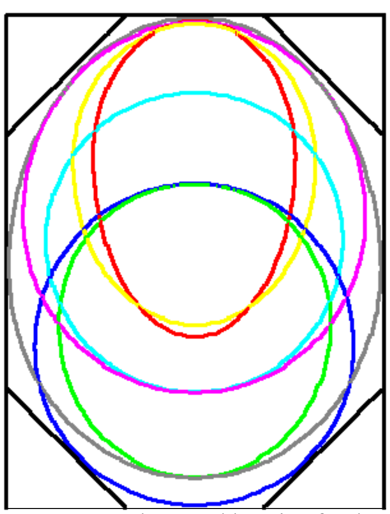

Figure 1: Beam shape and location for the seven bounces through the trap, superimposed on the schematic of a single detector.

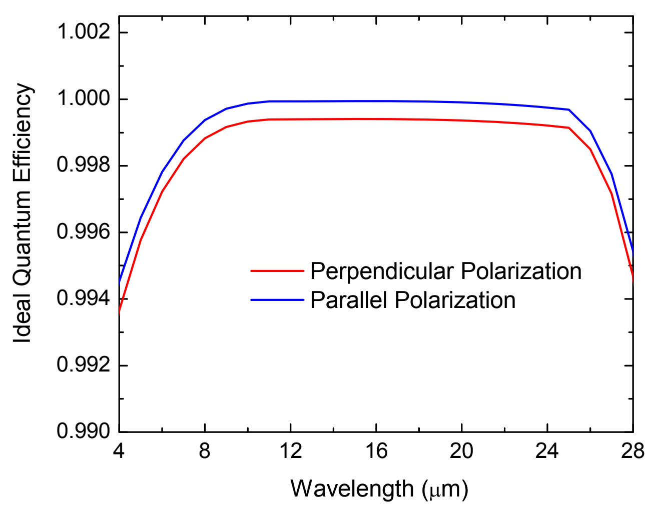

Figure 2: Estimate for the quantum efficiency of the BIB trap, assuming that the BIB devices from which it is composed have typical absorptivity values, and that there is nearly no internal loss.

trap mount. Leads from the flex circuit can be soldered to another electronics board from where the detector signal can be amplified. Figure 3 is a photo of the entire trap assembly as mounted in one of our cryostats.

3. EXPERIMENTAL PROCEDURE

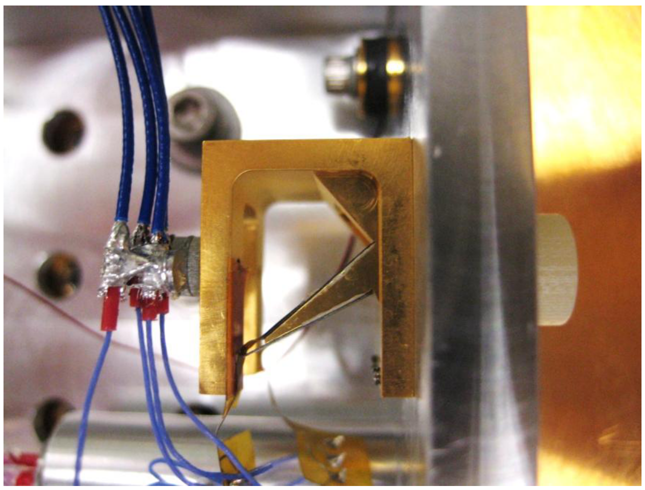

Figure 3: Photo of the BIB trap assembly from the side, as mounted in the FTS measurement cryostat.

BIB devices custom-designed for low internal loss were fabricated for use in the BIB trap detector. The main novel feature of these BIB detectors was that the silicon substrate on which they were grown was polished away after fabrication of the detector was complete, as shown in Figure 4. In the typical backside-illuminated BIB detector, there are internal losses associated with passage of the signal through the growth substrate, which is usually hundreds of micrometers thick. Profilometer measurements of the completed detectors show they are approximately 80 μm thick, and SIMS measurements show that the As doping concentration is approximately 1.7×10^{18} cm^{-3}. Cryogenic measurements show that the dark current of the BIBs designed for the trap is approximately 100 nA at a temperature of 9 K. A photo of the frontside of the BIB is shown in Figure 5, displaying the detector geometry, guard ring and wirebond pads.

Two separate measurement techniques were used to calibrate the internal spectral responsivity of the new BIB devices and the trapping detectors made from them. In the first technique, a Fourier-transform spectrometer was used to compare the responsivity of the BIB devices with that of a calibrated pyroelectric reference detector, providing very high resolution spectral information from 3 μm to 17 μm. In the second technique, the BIB trap response was compared in-situ within one of our calibration chambers with a primary standard absolute cryogenic radiometer (ACR). This measurement provided low uncertainty data with low spectral resolution over the range 5 μm to 11 μm, which can be used to verify the absolute scale of the responsivity determined by the high spectral resolution FTS measurement.

The FTS measurement was accomplished with our BIB detectors cooled within a small, mobile liquid helium cryostat and the signal from the FTS fed into the cryostat using an infrared optical fiber. The AgCl:AgBr optical fiber transmits well between 3 μm and 17 μm and its full output, under identical optical conditions, was measured by the BIB device within the cryostat and by the calibration pyroelectric detector in ambient. A schematic of the measurement technique is shown in Figure 6. An infrared globar source was used for all measurements and the comparison of the detectors was conducted in step scan mode because the response time of the pyroelectric detector was

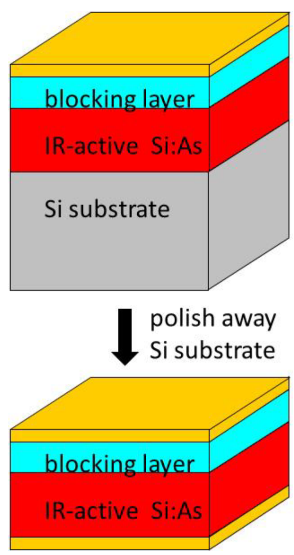

Figure 4: New custom-designed BIBs have the silicon growth substrate polished away to reduce internal losses.

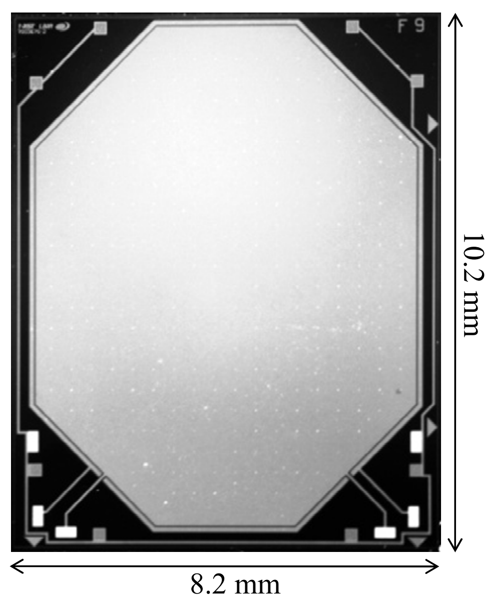

Figure 5: Photo of the frontside of the BIB device custom-designed for the BIB trap.

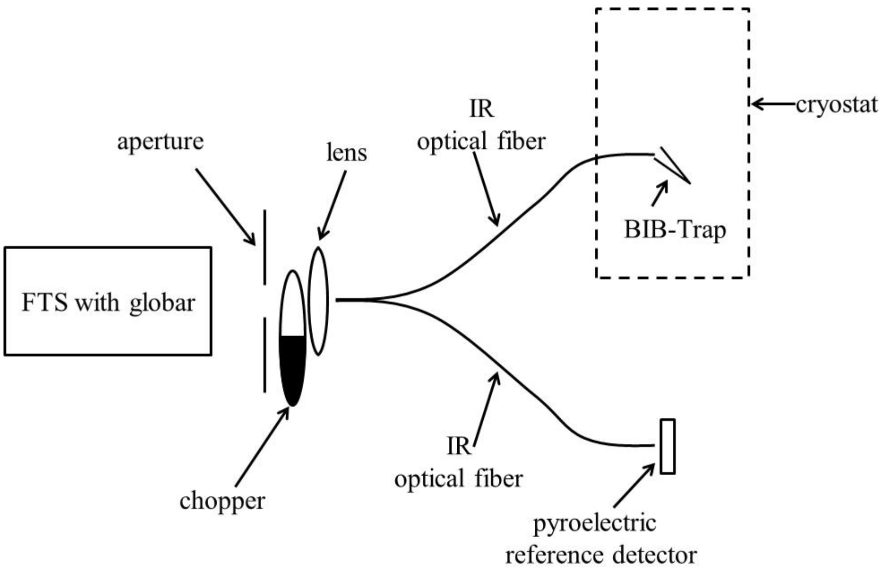

Figure 6: Schematic of the FTS measurement technique for calibrating the BIB trap against a pyroelectric reference detector.

approximately 0.01 s. Once the data on both detectors had been acquired, the ratio of the BIB detector data and the scaled pyroelectric data could be taken to find the responsivity of the BIB detector in units of A/W. This responsivity was then scaled by the ideal responsivity (λe/hc) to determine the quantum yield of the BIB detector or trap. Rapid scan FTS data with higher spectral resolution were also acquired for the BIB devices so etalon effects on the BIB responsivity could be analyzed.

Comparison of the BIB trap response with that of a primary standard ACR inside a NIST calibration chamber provided data with lower absolute uncertainty [10-12], although this filter-based technique has much lower spectral resolution than the FTS technique. In these ACR measurements, the blackbody source and the detectors share the same cryogenic vacuum space, and the two detectors are moved on a linear stage to sample the source beam at the same location. A schematic of the measurement technique is shown in Figure 7 and a photo of the ACR and BIB trap mounted on the linear stage in the calibration chamber is presented in Figure 8. A filter wheel near the source allowed the spectral content of the beam to be limited to narrow bands of approximately 0.5 µm fullwidth around 5 µm, 6 µm, 7 µm, 8 µm, 9 µm, and 11 µm. In this way, the power of the beam could be directly determined by the ACR around each of these wavelengths and the current response of the BIB trap at the same wavelength could be used to calculate the responsivity of the BIB trap in A/W. The BIB trap responsivity thus

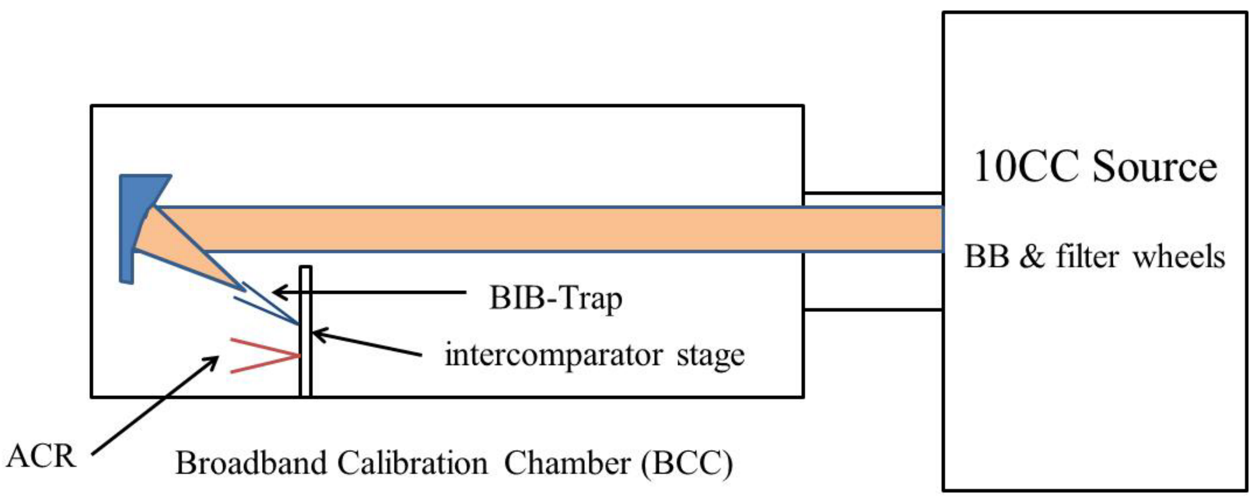

Figure 7: Schematic of the filter-based measurement technique for calibrating the BIB trap against a primary standard ACR detector. The blackbody source, filter wheels, and both detectors are located in the same cryogenic vacuum space.

determined could be used to verify and potentially scale the responsivity determined from the less accurate FTS technique.

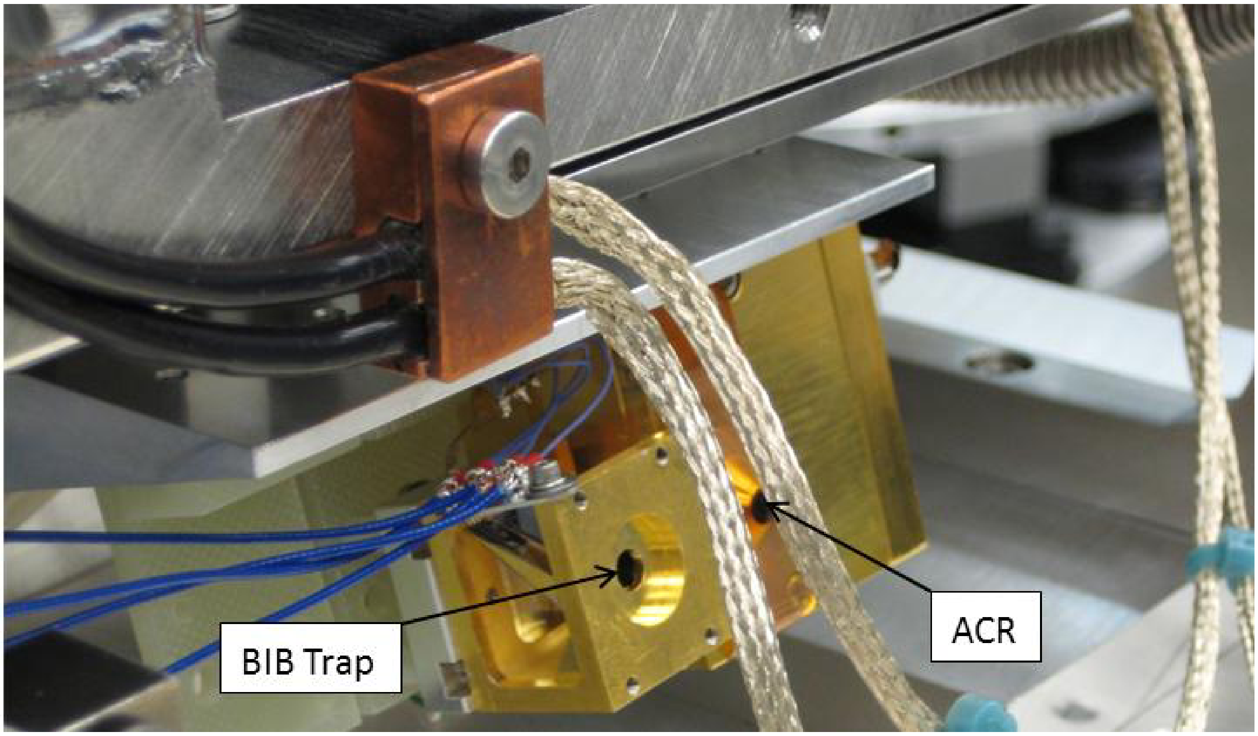

Figure 8: Photo of the BIB trap and ACR assemblies mounted next to each other on a linear stage inside one of our cryogenic vacuum calibration chambers.

4. EXPERIMENTAL RESULTS AND DISCUSSION

Analysis of the FTS calibration data for a single standard backside-illuminated BIB, a single new BIB custom-designed for the trap, and a BIB trap produce the quantum yield estimates presented in Figure 9 and Figure 10. In Figure 9, the quantum yield of a single BIB of the type utilized in the trap (measured at normal incidence) is compared with the quantum yield of a trap detector composed of such BIBs. As expected, the quantum yield of the trap is boosted significantly from that of the single BIB over the entire wavelength range measured. The quantum yield of the trap is not flat across the spectral range, however, and is lower than that estimated in Figure 2. The reason that the trap quantum efficiency does not reach its ideal value is evident in Figure 10, which compares the quantum yield of a single standard backside-illuminated BIB with that of a single BIB utilized in the trap. The quantum yield of the new detectors is significantly lower than that of a standard Si:As BIB, and although there is no loss in the new detectors due to a thick silicon substrate, there is evidence that a fabrication problem has led to less absorption within the infrared active layer than expected.

High spectral resolution FTS measurements prove that the trapping arrangement removes nearly all evidence of etalon from the spectral response associated with these BIB detectors. In Figure 11, the scaled responsivity of a single BIB and a trap made from two such BIBs is compared over the wavenumber range from 2000 cm^{-1} to 2800 cm-1 (5 μm to 3.57 μm). It can be clearly seen that the amplitude of the single BIB etalon is approximately 20 %, whereas the deviations from unity for the trap are approximately 2 %. The deviations for the trap do not have the regular period associated with the etalon of the single detector, so it is not clear whether the deviations for the trap are remnants of the etalon effects or may be from another source of measurement noise.

The responsivity results from the ACR/BIB-trap comparison show reasonable agreement with the BIB trap data from the FTS measurements. Figure 12 presents the quantum yield data from the ACR plotted as points from 5 μm to 11 μm,

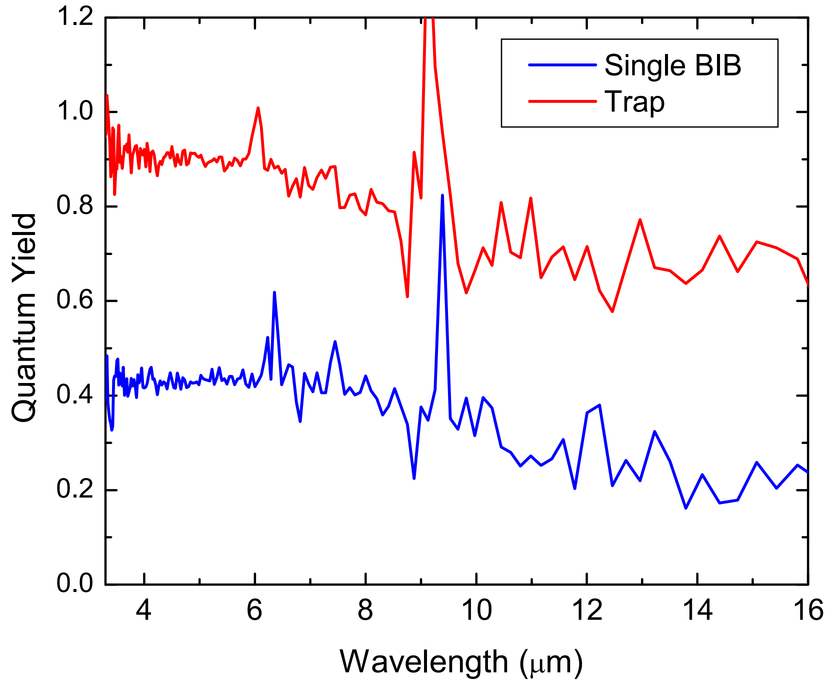

Figure 9: Comparison of the quantum yield for a single BIB and the quantum yield for a BIB trap fabricated from two such BIBs. The trapping configuration significantly raises the quantum yield over the entire spectral range. The data shown here has low spectral resolution so there is no evidence of etalon for either detector. Absorption in the IR optical fiber is responsible for the significant spectral feature seen near 9 μm.

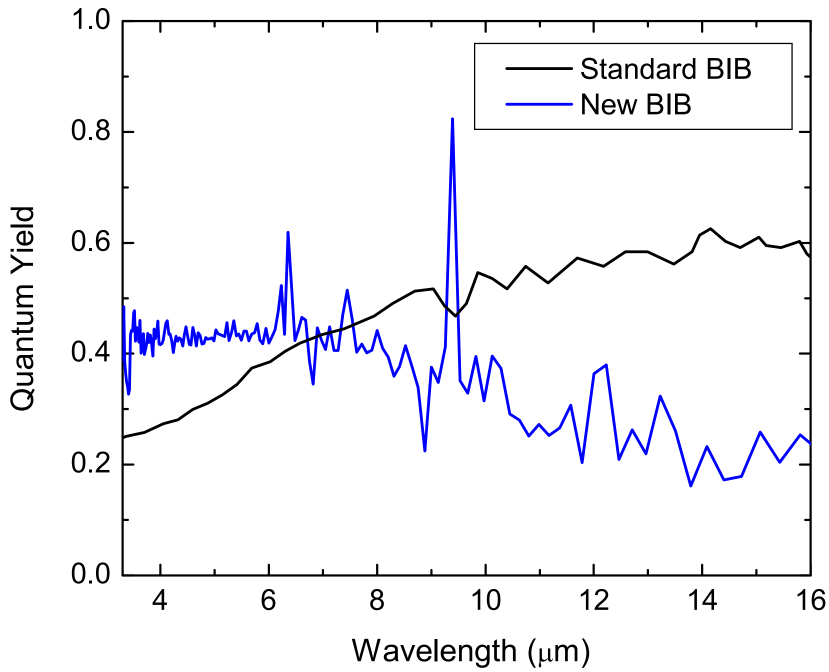

Figure 10: Comparison of the quantum yield for a single standard BIB and the quantum yield for a single new BIB custom-designed for low internal losses. Although the new BIB does not have loss associated with a thick silicon substrate, there is less absorption in the active layer than expected, particularly for the wavelengths longer than 8 μm.

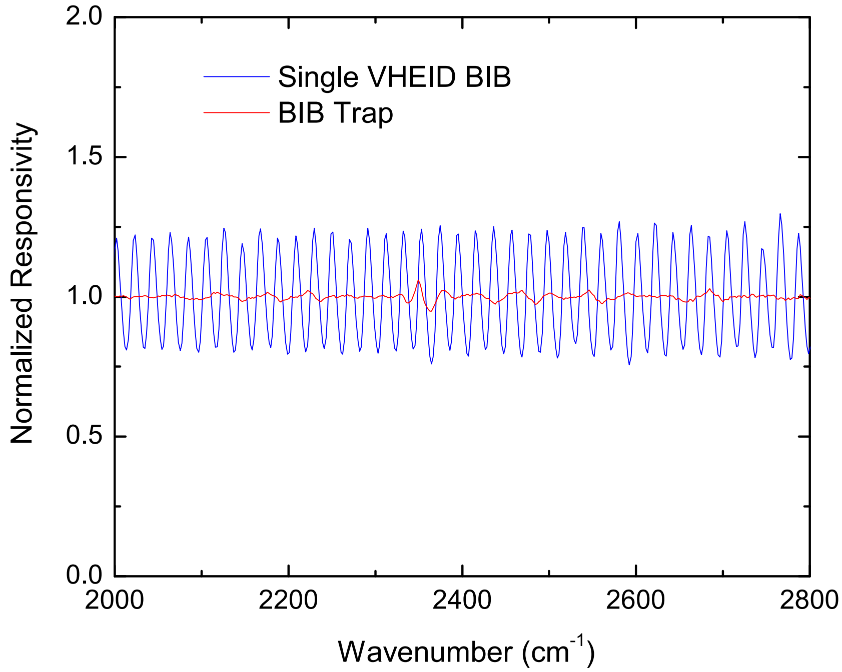

Figure 11: Comparison of the effects of etalon on the normalized responsivity for a single new BIB detector and a trap fabricated from two such BIBs, in the spectral range from 2000 cm^{-1} to 2800 cm^{-1}. Etalon produces oscillations with an amplitude greater than 20 % for the single BIB, but deviations are about 2 % in the case of the trap, and it is unclear whether these deviations are a result of etalon or a result of other sources of noise.

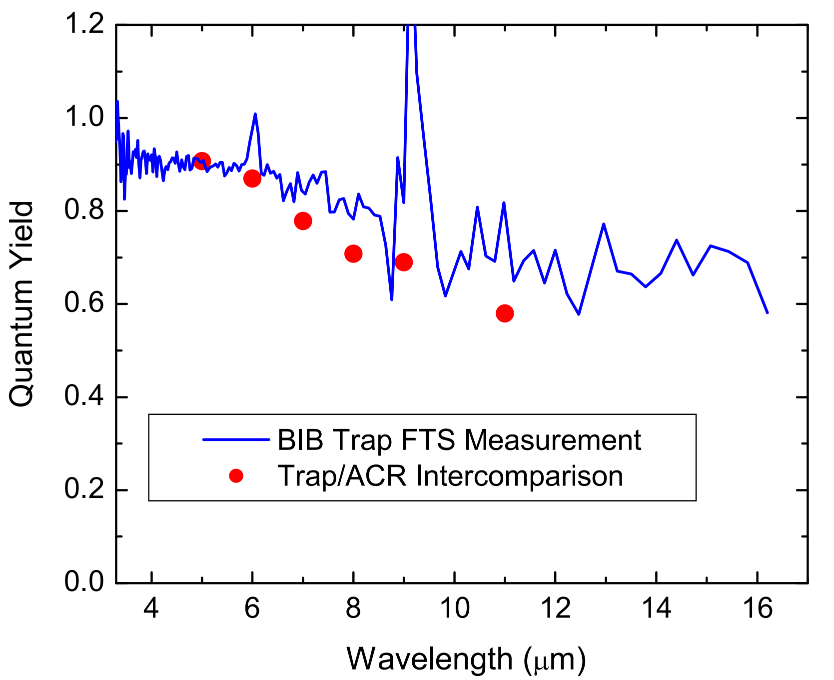

Figure 12: Comparison of the quantum yield of the BIB trap determined from the FTS measurement technique and from the filter-based ACR measurement technique.

along with the BIB trap quantum yield data from the FTS measurements. It can be seen that the two measurements agree well at short wavelengths but show a difference of up to 15 % at longer wavelengths. The maximum uncertainty is near the combined uncertainty associated with the FTS and ACR measurements. It should be noted that the BIB trap detectors measured by the two techniques were different, although the two BIB traps measured were constructed to be nominally identical.

Measurement uncertainty for the FTS technique is somewhat difficult to quantify, but is roughly estimated as ±10 % (k=1). The uncertainty in the raw data is estimated as ±2 % (k=1) for the BIB devices, ±5 % (k=1) for the pyroelectric detector, and ±2 % for the pyroelectric detector calibration. The FTS technique was also susceptible to uncertainty associated with parameters of the experimental set-up that could change with time or temperature because the BIB and pyroelectric measurements were made at different times and with different detector conditions. These ill-defined differences which could increase the uncertainties of the measurement include: changes in the beam from the FTS, changes in fiber acceptance or transmission from measurement to measurement, and change in fiber transmission with temperature. The uncertainty of the ACR comparison measurements is estimated at ±5% given the repeatability of the ACR and BIB measurements.

5. SUMMARY AND CONCLUSIONS

The responsivity of the BIB trap demonstrates improvements over the BIB devices from which it is fabricated. The spectral features from etalon are reduced in amplitude from approximately 20 % in the case of the single BIB to less than 2 % in the case of the trap. The quantum yield for the BIB trap shows significant improvement over the single BIB for the entire spectral range measured, although it does not yet show the ideal behavior illustrated in Figure 2. Reasonable agreement is seen between the FTS and ACR comparison data over the 5 μm to 11 μm range, lending credibility to the FTS results over their entire spectral range and for all the BIB devices measured. The quantum yield of the BIB trap could be increased by improving the properties of the single BIBs from which it is fabricated. One potential solution is to reprocess the BIBs custom-designed for this trap detector project in order to improve their properties. Another potential solution is to use standard backside-illuminated BIBs for a trap, accepting that there will be a guaranteed absorption loss from the silicon substrate on the order of 10 %. As realized thus far, the BIB trap has been demonstrated as a spectrally smooth detector between 3 μm and 17 μm with a quantum yield between 0.9 and 0.6.

* The authors would like to thank George Eppeldauer and Slava Podobedov for use of the pyroelectric reference detector and the monochromator-based calibration of its responsivity. We would also like to thank Boris Wilthan for the FTS-based calibration of the pyroelectric reference detector reflectance.

6. REFERENCES

[1] M.D. Petroff and M.G. Stapelbroek. *Blocked impurity band detectors*. United States Patent No. 4,568,960, filed October 23, 1980, granted February 4, 1986.

[2] Randall D. Campbell. *Characterization of the Si:As Blocked Impurity Band (BIB) detector in Keck's Long Wavelength Spectrometer (LWS)*. Experimental Astronomy **14** 57 (2002).

[3] A.K. Mainzer, Henry Hogue, Maryn Stapelbroek, Dale Molyneux, John Hong, Mike Werner, Michael Ressler, Erick Young. *Characterization of a megapixel mid-infrared array for high background applications*. High Energy, Optical and Infrared Detectors for Astronomy III (eds. David A. Dorn and Andrew D. Holland). Proc. of SPIE **7021**, 70210T (2008).

[4] B.L. Cardozo, E.E. Haller, L.A. Reichertz and J.W. Beeman. *Far infrared absorption in GaAs : Te liquid phase epitaxial films*. Appl. Phys. Lett. **83** (19) 3990 (2003).

[5] Adriaan C. Carter, Steven R. Lorentz, Timothy M. Jung, Beverly J. Klemme and Raju U. Datla. *NIST Facility for spectral calibration of detectors: calibration of arsenic doped silicon blocked impurity band detectors*. Infrared Detectors and Focal Plane Arrays VI (eds. Eustace L. Dereniak and Robert E. Sampson). Proc. of SPIE **4028** 420 (2000).

[6] Timothy M. Jung, Adriaan C. Carter, Steven R. Lorentz and Raju U. Datla. *NIST-BMDO Transfer Radiometer (BXR)*. Infrared Detectors and Focal Plane Arrays VI (eds. Eustace L. Dereniak and Robert E. Sampson). Proc. of SPIE **4028** 404 (2000).

[7] Adriaan C. Carter, Solomon I. Woods, Stephen M. Carr, Timothy M. Jung, Raju U. Datla. *Absolute cryogenic radiometer and solid state trap detectors for IR power scales down to 1 pW with 0.1% uncertainty*, Metrologia **46** (4), S146 (2009).

[8] Enrique J. Iglesias, Allan W. Smith and Simon G. Kaplan. *A sensitive, spatially uniform photodetector for broadband infrared spectrophotometry*. Applied Optics **47** (13) 2430 (2008).

[9] Max Born and Emil Wolf. Principles of Optics (Fifth Edition). Pergamon Press (Oxford), pp. 323-329, 1975.

[10] R.U. Datla, K. Stock, A.C. Parr, C.C. Hoyt, P.J. Miller and P.V. Foukal, "Characterization of an absolute cryogenic radiometer as a standard detector for radiant-power measurements," Appl. Opt. **31**(34), 7219-7225 (1992).

[11] J.M. Houston and J.P. Rice, "NIST reference cryogenic radiometer designed for versatile performance," Metrologia **43,** S31-S35 (2006).

[12] Adriaan C. Carter, Steven R. Lorentz, Timothy M. Jung and Raju U. Datla, "ACRII: Improved absolute cryogenic radiometer for low background infrared calibrations," Appl. Opt. **44**(6), 871-875 (2005).